



Spatio-temporal analysis of dry and wet periods in Iran by using Global Precipitation Climatology Center-Drought Index (GPCC-DI)

Alireza Hosseini¹ · Yousef Ghavidel¹ · Ali Mohammad Khorshiddoust² · Manuchehr Farajzadeh¹

Received: 11 April 2020 / Accepted: 10 November 2020 / Published online: 24 November 2020
© Springer-Verlag GmbH Austria, part of Springer Nature 2020

Abstract

In this study, the temporal and spatial characteristics of droughts in Iran, including severity, duration, frequency, and extent, were studied using the GPCC-DI, in a 68-year period from 1952 to 2019. To display and analyze these features, time trend components, intensity, duration, and area diagrams, Mann-Kendall non-parametric test and Kriging geostatistical method were used. The result of plotting intensity-duration-frequency maps shows an increasing trend in regional drought severity and spread. It was also found that the most severe droughts occurred in the 12- and 24-month periods from 2000 onward. Mann-Kendall test results also show that significant increases in droughts occurred in the central desert basins of Hamoon basin and south Baluchistan in the southeastern Iran. In addition, decrease in occurrences of dry and wet periods happened in the western, northwestern, and coastal regions of the Caspian Sea. The pattern of spatial variations of drought severity indicated two major drought foci in southeast and central Iran. The number of drought centers in Iran has also increased over time. The results of the analysis of the time trends of dry and wet periods point to the occurrence of continuous droughts in 12- and 24-month periods.

1 Introduction

Drought is one of the most common natural hazards that has profound effects on ecosystems, hydrology, agriculture, and the economy (Vicente-Serrano et al. 2012; Narasimhan and Srinivasan 2005). Understanding the spatial and temporal characteristics of drought is important in reducing the impacts and managing its risk (Mishra and Singh 2010; He et al. 2011). Therefore, drought as a spatio-temporal process is usually characterized by its intensity, spatial extent, and duration on a regional scale (Xu et al. 2015). This regional phenomenon sometimes covers large areas of land (WMO 2006).

Drought is more important in arid regions of the world and has led to many historical crises (Mishra and Singh 2010; Sheffield and Wood 2011; Tallaksen and Van Lanen 2004). Due to the importance of this issue, the study of this phenomenon in Iran has attracted the researchers' attention due to its greater necessity.

A plethora of studies have been conducted with regard to drought, and each of them have studied this issue from different aspects, e.g., Parry et al. (2010) who studied the spatio-temporal development and characteristics of large-scale droughts in Europe and Potop and Mozny (2011) who examined the new SPEI drought index in the Czech Republic and emphasized its ability to assess the severity of drought. Also Livia et al. (2014) evaluated the SPI and SPEI drought indices using COSMO model data in two Slovak watersheds and concluded that there was little correlation between these indices on a quarterly scale. Tomros and Menzel (2014) addressed the drought conditions under current and future climates in the Jordan River region located in the southeastern Mediterranean area and concluded that the 6-month SPEI drought index had the highest correlation with simulated soil moisture. Ziese et al. (2014) evaluated drought in Europe and parts of Asia. Their study showed that European droughts coincided with heat waves and increased evapotranspiration. Stage et al. (2015) also compared the frequency distributions of the SPI and SPEI drought indices in Europe. They recommended the two-parameter gamma distribution for general use when calculating SPI and the generalized extreme value distribution when computing the standardized precipitation evapotranspiration index (SPEI). Jianqing et al. (2016) analyzed the spatio-temporal characteristics of drought in China using SPI. Jin Um et al. (2017), using the SPEI index, studied

✉ Yousef Ghavidel
ghavidel@modares.ac.ir

¹ Department of Physical Geography, Tarbiat Modares University, Tehran, Iran

² Department of Climatology, University of Tabriz, Tabriz 51664, Iran

droughts in East Asia, Europe, the USA, and West Africa and showed that East Asia and West Africa had the highest drought intensity. Shah et al. (2015), using the 40-year precipitation data, monitored the drought in Surat, Gujarat, India on a 12-month scale using the standardized precipitation index (SPI).

In Iranian context, Doostan (2020) analyzed 403 scientific research articles published in the years 2000 to 2017 in Iran and found that 78% of the conducted studies had only assessed drought in different parts of Iran and these assessments have been at the regional, watershed, or station scales. Eleven percent of drought articles investigated the consequences of this climatic phenomenon in various sectors including water, agriculture, social harms, and so on. Also, about 7% of drought studies aimed to predict this phenomenon with different statistical models, and 2.5% of drought studies focused on drought management and zoning in different regions of Iran.

Raziei et al. (2011) focused on the spatial analysis of drought in Iran using GPCC and NCEP/NCAR networked data through applying principal component analysis (PCA) method. The results of their research were compared with observations in 32 precipitation assessment stations and showed that GPCC datasets had high accuracy for drought analysis and could yield useful data for drought.

Babae and Alijani (2013), with data from seventy stations that had a statistical period of 30 years and more, and using SPI index in 12- and 24-month periods, studied drought in Iran. Their results showed that in a 12-month period, droughts were very severe in east, southwest, west, and center of the country, but in the northeast, northwest, and north of the country, droughts were moderate and mild. During the 24-month period, the droughts in the west, east, southeast, south, and center of the country were very severe.

Keshavarz et al. (2012) evaluated the distribution pattern of the direction and intensity of drought changes in Iran using the Palmer drought severity index for a period of 36 years (1975–2010) using networked soil and meteorological data. To observe the pattern of severity and trend of drought, they used linear regression method with a time step of 1 month as a spatial distribution. The calculation results showed that more than 60% of the study area had a negative trend (increasing drought) and less than 4% had a negative trend (wet year improvement) which were significant at the level of 5%. Farajzadeh and Ahmadian (2014) analyzed the spatio-temporal characteristics of drought using the SPI index and investigated the temporal and spatial patterns focusing on three characteristics of severity, frequency, and duration in Iran. Shokoochi and Morovati (2014) investigated Urmia Lake basin drought using the standardized precipitation index (SPI) and reconnaissance drought index (RDI). Their data for analysis including precipitation and temperature were provided from two global databases: GPCC for precipitation and

NCEP/NCAR for temperature. Their study showed that since 2000, the basin has approached normal conditions in terms of both rainfall and drought, but the area of Urmia Lake has continued its declining trend to this day. Ghorbani et al. (2019) using SPI climate drought index evaluated the drought trend of Esfahan province using non-parametric tests of Sens, Pettitt, and Mann-Kendall for a statistical period of 27 years (2017–2011). Their results showed a meaningful downward trend at a significance level of 5%. It also showed that analysis of drought time series for longer than 6-month index better expresses the trend of change than short time series.

In this study, unlike previous research, which only studied drought on a stationary basis, wet and dry periods are studied together regionally so that we could evaluate the spatial changes of wet and dry times and extract their concentrations.

2 Material and methods

2.1 Study area

Iran, with an area of 1,648,195 km², lies between 25 to 39° northern latitudes and 44 to 63 eastern longitudes, in the region of air subsidence and stability of air, and is one of the subtropical and arid zones. Being located in the arid and semi-arid belt of the world has caused large parts of the country to be subject to repeated droughts. The geographical position of the study area is shown in Fig. 1.

3 Theoretical basis and methods

This study has used the data of Global Precipitation Climatology Center-Drought Index (GPCC-DI) from the GPCC database, established by the WMO and administered by the German Meteorological Agency. The GPCC analyzes the monthly precipitation that reaches the Earth's surface. This database makes precipitation data available for the entire surface of the Earth except the water-covered areas. An important advantage of this global database is that it provides users with networked data. The database uses temperature data provided by the NOAA Climate Prediction Center to calculate wet season and droughts applying the GPCC-DI index and provides users with the data. The networking of this database is based on latitude and longitude, which is available with a resolution of 0.5×0.5 , 1×1 , and 2.5×2.5 degrees. These data involve calculating SPI and SPEI indices as average monthly precipitation and networking data for average monthly temperature. The GPCC-DI drought index is based on average monthly networked rainfall and temperature. Initial estimation data are usually available from the GPCC Center 3 to 5 days after the end of each month. These data are available based on synoptic reports (weather forecast) with a regular network

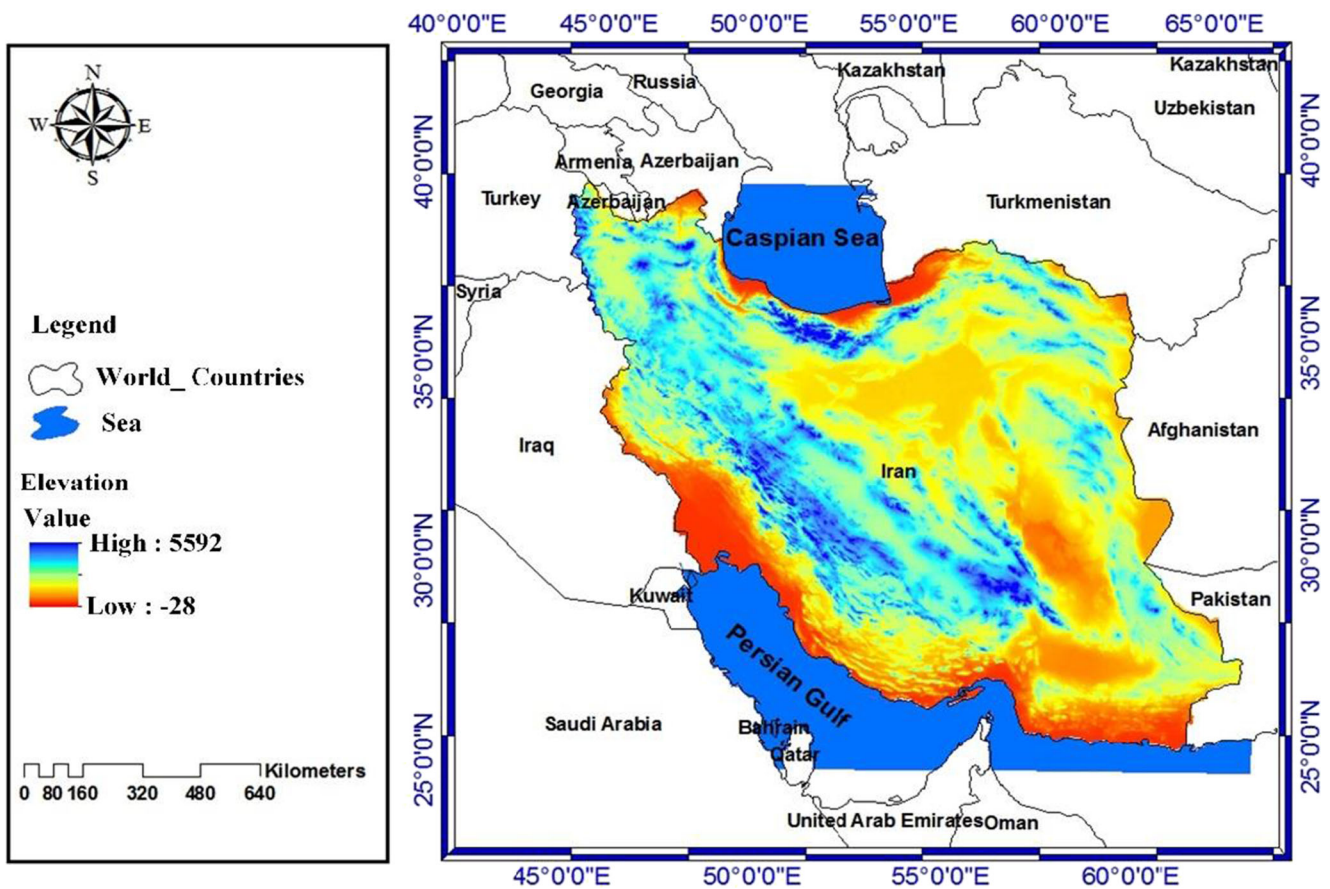


Fig. 1 Geographical location and topographical map of Iran

with different spatial resolutions. Data with a spatial resolution of 1*1 degree in the time period of 1952 to 2019 were used in this research. GPCC-DI index first calculates SPI and SPEI indices, and then GPCC-DI is calculated using the average of both indicators for each cell of the network. After mapping and extracting SPEI features, each data cell was ordered in terms of year, and changes in time series of data were calculated by using Mann-Kendall non-parametric method for testing of the trend (Tao et al. 2011).

3.1 Calculation of the drought indices

3.1.1 Standardized precipitation index

The SPI is an index based on the probability of precipitation used for different time scales. It also predicts the occurrence of drought conditions prior to its incidence and helps estimate the drought severity and is less complex than the Palmer drought severity index (PDSI). The calculation of the SPI for each region is based on the long-term precipitation data record for an arbitrary period. These long-term precipitation reports are fitted to a probability distribution, so the mean standardized precipitation for each region and for each arbitrary period is zero, and its standard deviation is one.

Positive values of the SPI are better representatives than average precipitation, while negative values of this index are lower representatives than average precipitation. Since the SPI is numerical, it can be the same both in dry and humid climates, and wet periods can also be represented through this index.

The SPI is derived from the following equation:

$$SPI = \frac{P_i \pm \bar{P}}{S} \tag{1}$$

where:

- P_i the amount of rainfall in the study period
- \bar{P} average long-term rainfall for the study period
- S standard deviation of precipitation

3.1.2 Standardized precipitation evapotranspiration index

This index was first introduced by Vicente-Serrano et al. (2010). SPEI is a multi-scalar index in which precipitation and temperature data are combined. Its calculations are similar to the SPI. In SPI, the input data are monthly or weekly precipitation values, but in SPEI, the same data along with PET values are used. Thus, in fact, SPEI captures the main impact

of increased temperatures on water demand. The first step to calculate SPEI is difficult due to the calculation of various parameters including surface temperature, air humidity, soil incoming radiation, water vapor pressure, and ground-atmosphere latent and sensible heat fluxes. Differential methods of the amount of evaporation and perspiration from the parameters measured at the meteorological station are estimated indirectly. Based on the available data, physical methods (Penman–Monteith method: PM) and experimental methods are used to calculate PET with lesser parameters. Mavromatis (2007) showed that using complex methods to calculate PET had similar results in determining PDSI. Although the SPI can be calculated using two-parameter distribution, such as the gamma distribution, the distribution of the three parameters is required to calculate the SPEI. In the distribution of two parameters, the variable x has a lower limit of zero ($0 < x < \infty$), while in the distribution of the three parameters, x can take values in the range ($\gamma < x < \infty$), where γ is the parameter origin of the distribution; consequently, x can have a negative value, which are common in D series.

The probability distribution function of the D series, according to the log-logistic distribution, is given by:

$$F(x) = \left[1 + \left(\frac{\alpha}{x-\gamma} \right)^\beta \right]^{-1}, \tag{2}$$

The $F(x)$ values for the D series at different time scales adapt very well to the empirical $F(x)$ values, independently of the climate characteristics and the time scale of the analysis. The suitability of the log-logistic distribution to model $F(x)$ values from the D series in each region of the world has been proven (Singh et al. 1993). The SPEI can easily be determined by the standardized values of $F(x)$.

Following the classical approximation of Abramowitz and Stegun (1965), the SPEI is determined as follows:

$$\text{SPEI} = W - \frac{C_0 + C_1W + C_2W^2}{1 + d_1W + d_2W^2 + d_3W^3} \tag{3}$$

where w is calculated from the following equation:

$$W = \sqrt{-2\ln(P)} \quad \text{for } P \leq 0.5$$

and P is the probability of exceeding a determined D value, $P = 1 - F(x)$. If $P > 0.5$, then P is replaced by $1 - P$, and the sign of the resultant SPEI is reversed. The constants in the above formula are as follows: $C_0 = 2.515517$, $C_1 = 0.802853$, $C_2 = 0.010328$, $d_1 = 1.432788$, $d_2 = 0.189269$, and $d_3 = 0.001308$.

The average value of SPEI is 0, and the standard deviation is 1. The SPEI is a standardized variable and can therefore be compared with other SPEI values over time and space. An SPEI of 0 indicates a value corresponding to 50% of the

cumulative probability of D , according to a log-logistic distribution (Vicente-Serrano, 2010) (Table 1).

Also, to analyze maps of spatial distribution of the droughts and wet periods, the Kriging method was selected from different geostatistical and algebraic methods, based on statistical tests and semi-variogram analysis, due to its lower level of error.

4 Results and discussion

4.1 Intensity-duration-frequency analysis

In the GPCC_DI method, monthly precipitation was embedded in a grid field with a resolution of 1×1 that covered the whole of Iran with 157 cells. Each cell represented the SPEI value calculated; networks with SPEI below 1 (moderate or severe drought) were identified and assigned to the drought category. Starting from the network with the lowest SPEI (maximum drought severity), adjacent networks (neighboring networks) were taken into consideration if they belonged to the drought category. This method was repeated as long as there was no network adjacent to the current cluster of drought-related networks. If drought networks existed outside the current cluster, a new cluster would be created by using the above method, for example, SPEI of the cells that were between 0 and 1 were in the wet cluster. At the end, separate drought clusters with different sizes of the adjacent area were identified for a specific time step (e.g., 3 months). The drought intensity of each cluster was defined as the mean SPEI of all networks in the cluster.

To produce drought duration curves for 3, 6, 9, 12, and 24 months, which were previously defined, drought was first identified with period t (time step i represents the time interval i to $i + t - 1$) in each network, for each time step. The severity of the drought (I) was then defined as $I = \Sigma \text{SPEI} / t$, where ΣSPEI is accumulated over a period of t for each network. For each step of stage I, the curve analysis was based on the clustering algorithm, which began with a network with the lowest SPEI value. With the connection of neighboring networks with low SPEI values in the drought sector, area and

Table 1 SPEI drought index categories (Jianqing Zhai, 2016)

Status	Percentage of normal
Extremely wet	2 and above
Very wet	1.5 to 1.99
Moderately wet	1 to 1.99
Near normal	0.99 to -0.99
Moderately dry	-1 to -1.49
Severely dry	-1.5 to -1.99
Extremely dry	and less -2

intensity were calculated and recorded on the basis of the aggregated area of the network, and the average intensity until the maximum spatial extent of the drought event was reached. As can be seen in Fig. 2, the intensity, duration, and frequency of drought for the years 1952 to 2019 were calculated using the numerical value of each cell. Intensity, duration, and frequency diagrams were calculated for defined periods of 3, 6, 9, 12, and 24 months, respectively.

As shown in the intensity-duration-frequency diagrams (Fig. 3), dry and wet events were calculated according to their trends in intensity and time periods. The spatial distribution of trends of dry and wet period trends over the study period (1952 to 2019) showed incremental trends in drought severity. As can be seen in Fig. 3, the change trend and intensity of droughts have changed drastically, and the total area affected by the drought has increased significantly from 1952 to 2019. In recent years, especially since the 2000s, the intensity and frequency of 12- and 24-month droughts have increased

dramatically. In addition, the extent of the area affected by severe droughts, particularly extremely severe droughts, has increased intensely in the last decade. The most severe and widespread severe droughts were in the 12- and 24-month periods, which are much more pronounced in the post-2000 period. For example, in 2000, during the 24-month period, about 23 percent of Iran’s area was affected by severe droughts. In addition, droughts in the 2000s and 2010s have had two very sharp peaks. In general, the amount and intensity of wet periods in all the studied periods have declined sharply in recent years. But by 2015, the situation has returned to its normal condition. Wet periods had three peak phases, most of which had an increase in their regional extent in the 1950s, 1970s, and 1990s. Most of the wet periods were observed in the 1950s, especially in 1955, with approximately 50% of Iran’s area experiencing favorable wet periods. The highest humidity intensity or extremely wet season also occurred in 1955.

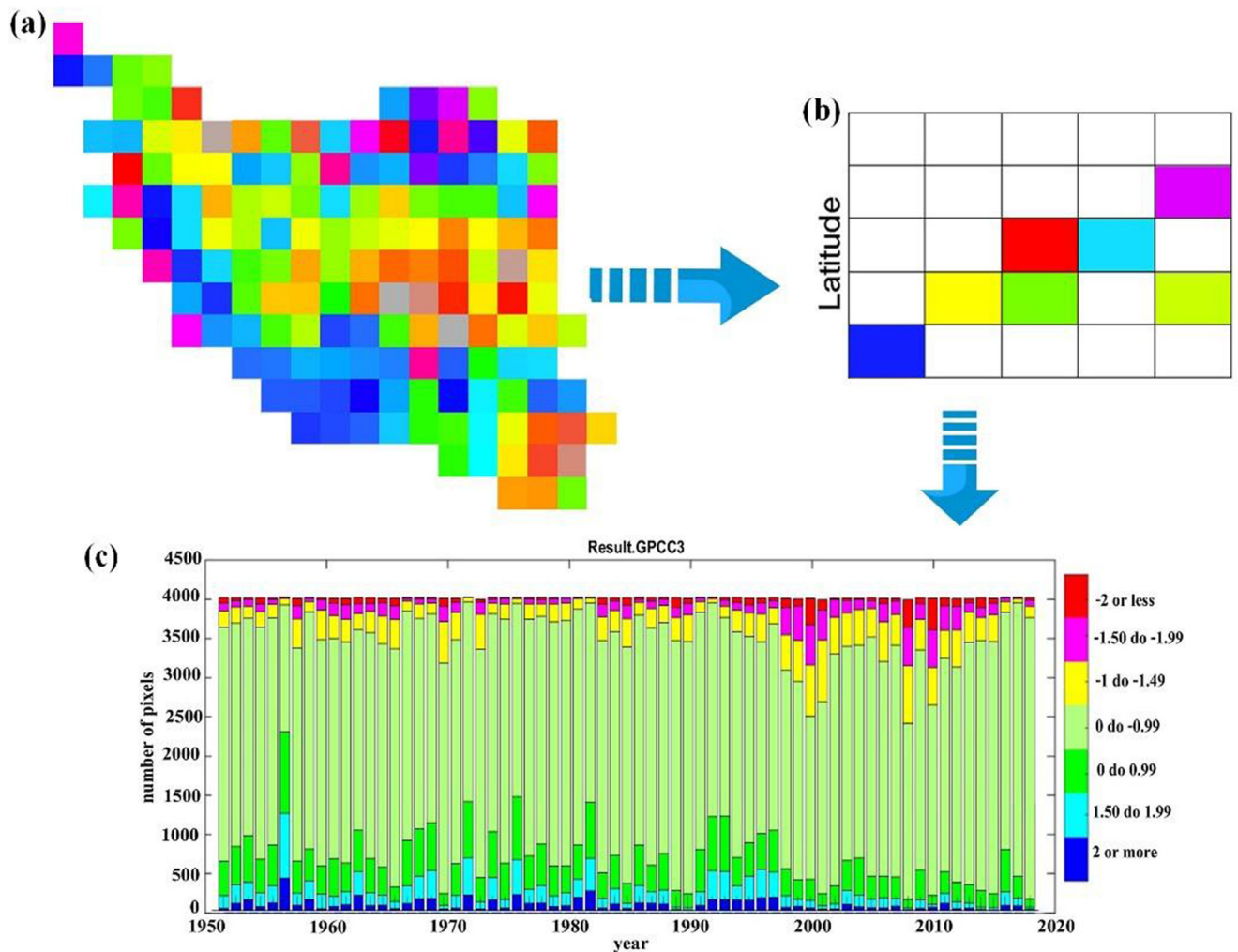
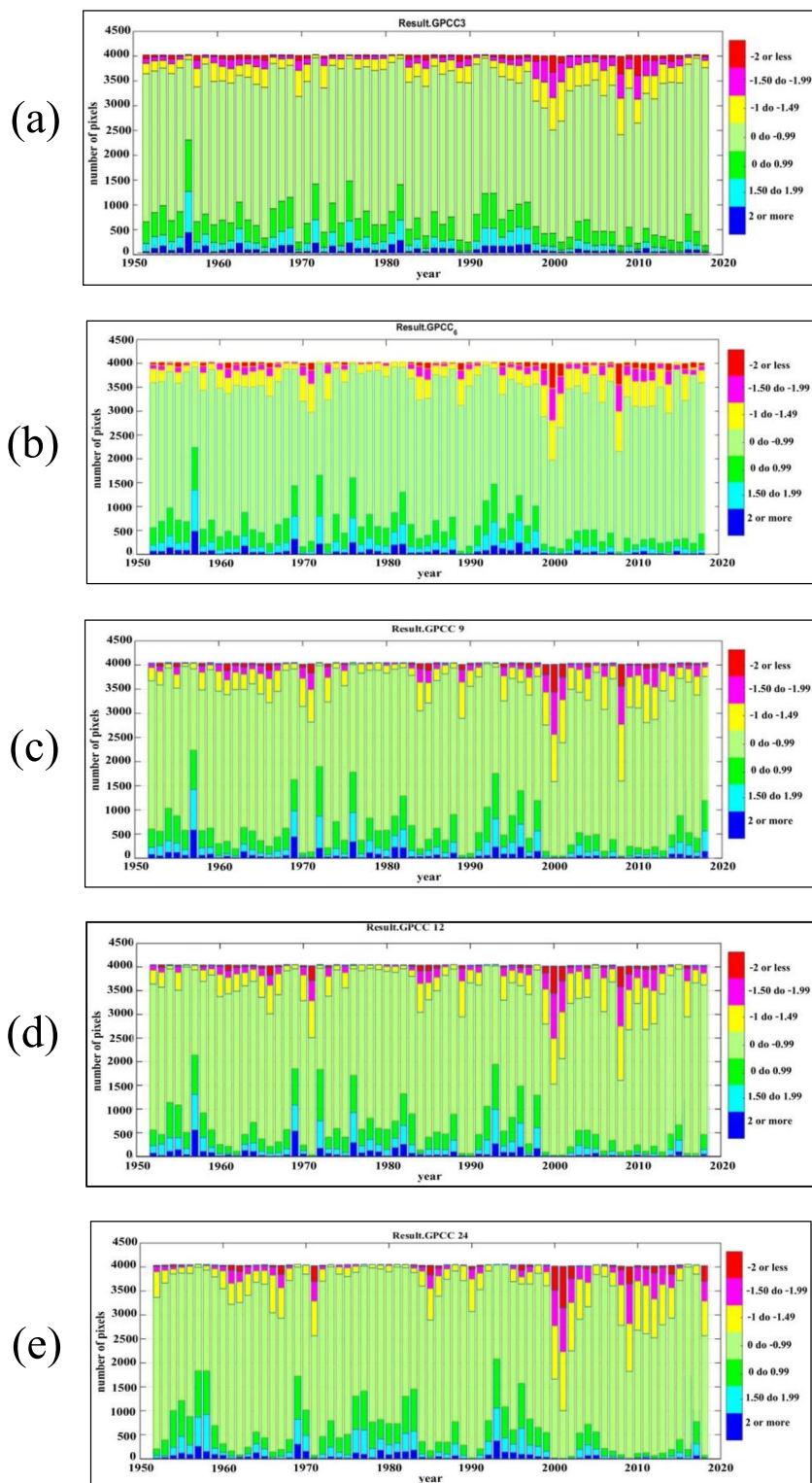


Fig. 2 The stages of the intensity-duration-frequency curves of dry and wet periods

Fig. 3 The intensity, duration, and frequency curves for (a) 3-month, (b) 6-month, (c) 9-month, (d) 12-month, and (e) 24-month periods, respectively



4.2 Detecting and analyzing temporal changes

The existence of trend in GPCC-DI time series was checked using Mann-Kendall test. To this purpose, we acted based on the classification of the primary catchments of Iran provided

by the Ministry of Energy, and the spatial patterns of GPCC-DI indices in positive or negative directions for the observed period from 1952 to 2019 are shown in Fig. 4.

The intensity and trend of the time periods show a significant increase in drought intensity in the central parts of Iran in

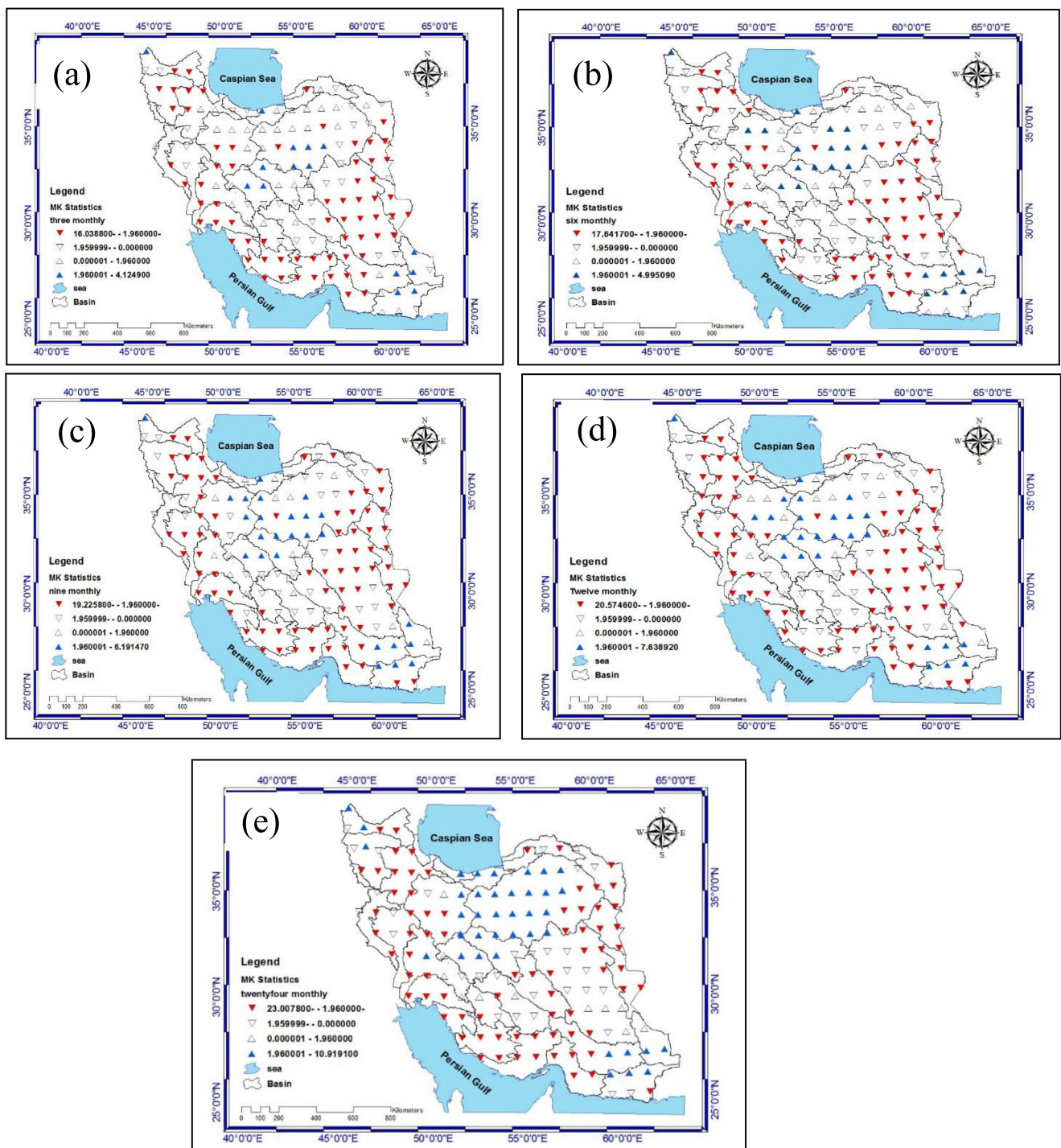
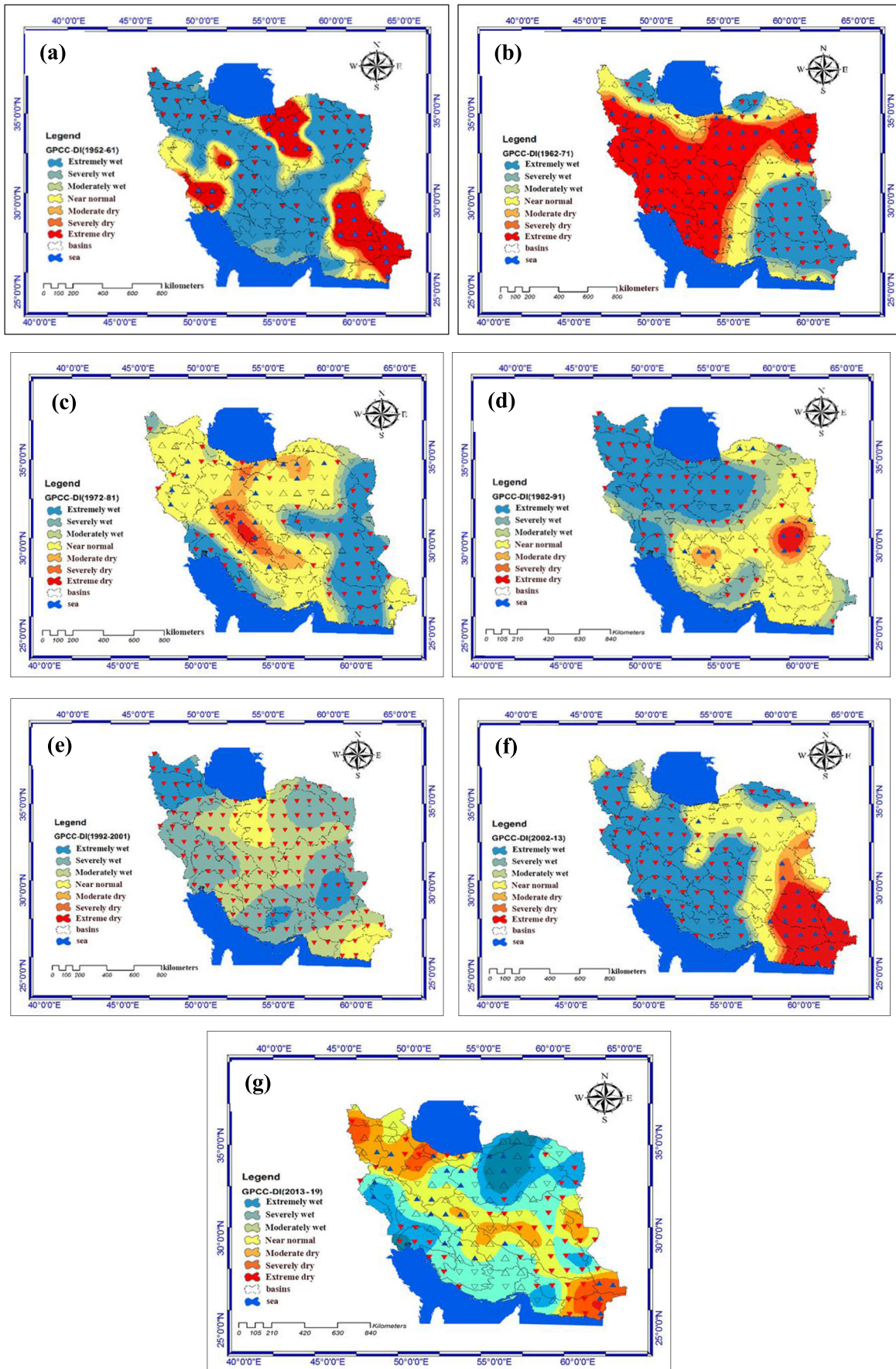


Fig. 4 Spatial distribution of trends for the studied period 1952–2019 (reversed red triangle indicates significant decline, and blue triangle indicates significant growing drought trend) for (a) 3-month, (b) 6-month, (c) 9-month, (d) 12-month, and (e) 24-month periods

the Central Desert, Siahkuh (Black Mountain) Desert, and Gavkhuni catchments in Qom, Semnan, Esfahan, and Yazd provinces and southeastern areas of Iran in Hamoon and Sistan and Baluchistan basins. Significant decreasing trends in the severity of droughts are also found in most of the western part of Iran, in the southern shores of the Caspian Sea, the northeast, and the southern coast of Iran in the Persian Gulf,

indicating significant positive trends and humid conditions. In addition, non-significant random trends are observed in Bakhtegan and Sefid Rood, Ghareh Ghom and Atrak basins in northeast and middle north of Iran, Darreanjir Desert, Sirjan Desert, and Bakhtegan in southern Yazd and northern Kerman and Fars show that these areas do not display significant trends.



◀ **Fig. 5** Spatial variation and intensity and direction of dry and wet season orientations for the studied period from 1952 to 2019 for a 12-month period (a) 1st decade, (b) 2nd decade, (c) 3rd decade, (d) 4th decade, (e) 5th decade, (f) 6th decade, and (g) 7th decade

Despite the concentration and stability of drought centers in the central and southeastern areas, in different periods of time, the number and intensity of droughts have increased, and the extent of the drought zone has expanded to the northern and northeastern regions of Iran.

4.3 Spatial variation and intensity of drought trends

The spatial patterns of approaches for the GPCC-DI index in Iran are shown in Fig. 5. Positive or negative trends and significant trends are calculated based on MK statistics in the form of 10-year period from 1952 to 2019. Intensity was calculated as a mean, and it is comparable with Mann-Kendall test.

Generally, in all statistical periods, there are two main drought foci, which include the central desert basin in central Iran and the Hamoon and southern Baluchistan basins in southeastern Iran, both of which show an increasing trend of drought intensity (Fig. 5). The trend and severity of droughts are extending from the southeastern part of Iran to the western and southwestern parts of Iran. Over time, drought foci have also increased in various parts of Iran, even in many areas with humid climates, such as the northern coastline and northwestern Iran; there was an increase in drought. The expansion of the drought foci from the southeast to the Bakhtegan and Maharloo watersheds in the southwest, and the Karun watersheds and parts of the Jarahi basin, respectively, is significant. In almost all studied time periods, the increasing trend of droughts is consistent with the occurrence of moderate to severe droughts, and the spatial patterns are very similar to those of severe droughts. The significant point of these maps is that of the 1990s, during which all the regions of Iran experienced a reduction in drought intensity. A decrease in drought severity also occurred more in the northwestern parts of Iran, which is observed almost in all periods.

4.4 Analysis of trends and drought and wet periods

The GPCC_DI mean criterion was calculated, and the time trend charts were plotted for 3, 6, 9, 12, and 24-month periods. As can be seen in Fig. 6, the time trends of the various indices show fluctuating and variable conditions throughout all periods. The rate of decline and increase in time trends for periods 3, 6, and 9 is almost unstable, and despite variations, it does not show a significant trend. During these periods, all dry and wet periods have occurred with little extent and coherence. During the 12- and 24-month periods, however, changes

have been much more intense, and in recent years, trends are more prone to severe droughts. In addition, in the time span of 12 and 24 months, there has been a dramatic increase in the extent of continuous droughts.

5 Conclusion

In this study, using intensity-duration-frequency diagram, Mann-Kendall test, time trend diagram, and Kriging geostatistical method, we analyzed the temporal variability status and long-term variations of Iranian dry and wet periods and their spatial patterns.

The spatial distribution of dry and wet period trends over the period under investigation (1952 to 2019) shows increasing trends in drought severity, with drought intensity changing relatively severely and the entire area significantly amplified under the influence of drought. The most severe and widespread droughts occurred in two 12- and 24-month periods. This trend has intensified dramatically since 2000, covering about 23 percent of the area. Wet periods have three peak periods, most of which had an increase in their regional area in the 1950s, 1970s, and 1990s. The greatest extent of area involved in wet periods was observed in the 1950s, especially in 1955.

Significant increases in drought intensity are observed in the central parts of Iran in the Central Desert, Siahkuh (Black Mountain) Desert, and Gavkhuni catchments in Qom, Semnan, Esfahan, and Yazd provinces and southeastern areas of Iran in Hamoon and Sistan and Baluchistan basins. Significant decreasing trends in drought severity were also observed in most areas of the western part of Iran, the southern coast of the Caspian Sea, and the northeast and the southern coast of Iran in the Persian Gulf.

Spatial patterns derived from the GPCC-DI index generally showed two major centers of droughts across two statistical periods, which include the central desert basin in central Iran and the Hamoon and Baluchistan basins in southeastern parts of Iran.

Both areas have an increasing trend in drought intensity. In general, the trend and severity of droughts in Iran extend from the southeast to the western and southwestern regions. Another important point is that the number of drought centers in different parts of Iran has increased over time.

Temporal analysis of the occurrence of droughts in Iran revealed that during the 12- and 24-month periods, the intensity of the changes has greatly increased, and trends are increasingly moving towards severe droughts in recent years. In addition, the duration of droughts and the number of continuous and prolonged droughts have increased over periods of 12 and 24 months.

Chronological analysis of the occurrence of droughts in Iran has shown that in the periods of 12 and 24 months,

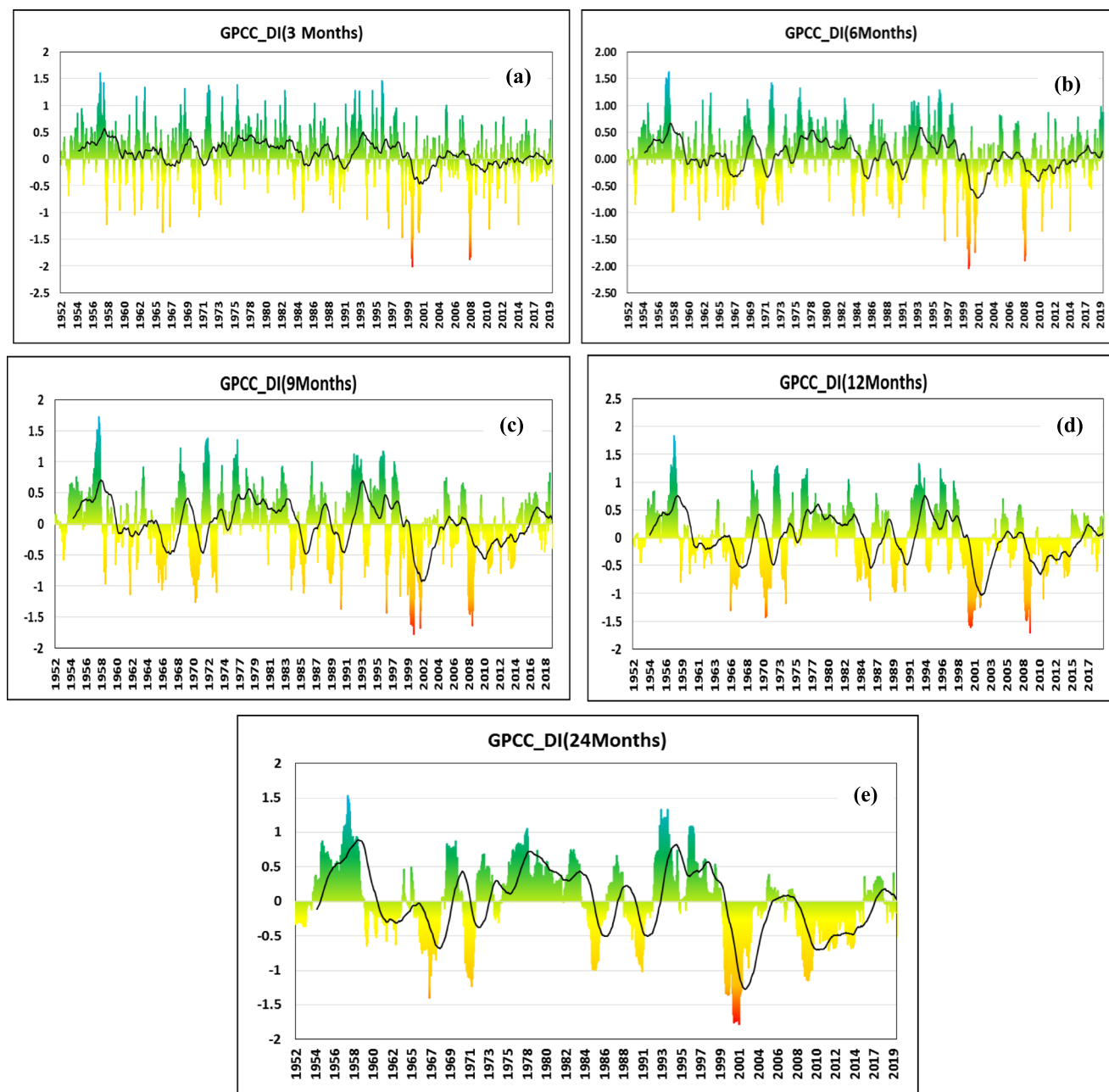


Fig. 6 The graph of long-term dry and wet season trends in (a) 3-month, (b) 6-month, (c) 9-month, (d) 12-month, and (e) 24-month periods over 1952–2019

the intensity of changes has increased significantly, and trends are moving more towards severe droughts in recent years. The results of this research are consistent with previous studies (Babaei and Alijani 2013; Keshavarz et al. 2012; Farajzadeh and Ahmadian 2014) that used station data to study drought in Iran and provide further details about drought over a longer period of time and a larger regional scale including the whole Iran.

Past research on drought and wet season has focused mainly on time series analysis of drought, and little attention has been paid to wet season changes. Also, in

this study, instead of a point (stationary) approach, a regional (zonal) approach was used to have a spatial analysis of dry and wet season and to study the spatial changes of areas affected by dry and wet season in Iran over a period of 67 years, which had not been previously studied. This study, due to the application of longer-term statistics and a newer and more accurate hybrid method, better exposes the temporal and spatial characteristics of dry and wet periods in Iran, and the resulting information will be useful for better drought management and better land preparation.

Author's contributions The authors' participations in the article are as follows:

Conceived and designed the analysis: Yousef Ghavidel and Alireza Hosseini

Collected the data: Alireza Hosseini and Yousef Ghavidel

Contributed data or analysis tools: Manuchehr Farajzadeh, Alireza Hosseini, and Yousef Ghavidel

Performed the analysis: Alireza Hosseini, Yousef Ghavidel, and Ali Mohammad Khorshiddoust

Wrote the paper: Alireza Hosseini

Writing—review and editing: Ali Mohammad Khorshiddoust

Supervision: Yousef Ghavidel

Corresponding author: Yousef Ghavidel

Compliance with ethical standards

Conflict of interest The authors declare that they have no conflict of interest.

References

- Abramowitz M, Stegun IA (1965) Handbook of mathematical functions, with formulas, graphs, and mathematical tables. Dover Publications, Mineola, p 1046
- Babae O, Alijani B (2013) Spatial analysis of long duration droughts in Iran. *Phys Geog Res Quarterly* 85:1–12. <https://doi.org/10.22059/jphgr.2013.35831>
- Doostan R (2020) Analysis of drought researches in Iran (2020). *J Spat Anal Environ Hazard* 6(4):2–2020. <https://doi.org/10.29252/jsaeh.6.4.53>
- Farajzadeh M, Ahmadian K (2014) Temporal and spatial analysis of drought with use of SPI index in Iran. *J Nat Environ Hazards* 3(winter 2014):1–16. <https://doi.org/10.22111/JNEH.2014.2464>
- Ghorbani H, Ali Vali A, Zarepour H (2019) Analysis of the climatological drought trend variations using Mann-Kendall, Sen and Pettit tests in Esfahan province. *J Spat Anal Environ Hazard* 6(2):9. <https://doi.org/10.29252/jsaeh.6.2.129>
- He B, Lü AF, Wu JJ et al (2011) Drought hazard assessment and spatial characteristics analysis in China. *J Geogr Sci* 21(2):235–249
- Jianqing Z, Jinlong H, Buda S, Lige C, Yanjun W, Tong J, Fischer T (2016) Intensity, area and duration analysis of droughts in China 1960–2013. Springer-Verlag, Heidelberg
- Keshavarz MR, Vazifedoust M, Fatahi E, Behyar MB (2012) Distribution pattern of direction and intensity of drought changes in Iran using Palmer drought intensity distribution index. *J Appl Res Geogr Sci* 27:98–101
- Livia L, Lukas S, Gunther H (2014) The comparison of the SPI and the SPEI using COSMO model data in two selected Slovakian river basins. EGU General Assembly, Vienna
- Mavromatis T (2007) Drought index evaluation for assessing future wheat production in Greece. *Int J Climatol* 27:911–924
- Mishra AK, Singh VP (2010) A review of drought concepts. *J Hydrol* 391:202–216
- Narasimhan B, Srinivasan R (2005) Development and evaluation of soil moisture deficit index (SMDI) and evapotranspiration deficit index (ETDI) for agricultural drought monitoring. *Agric For Meteorol* 133(1–4):69–88
- Parry S, Prudhomme C, Hannaford J, Hughes B (2010) Examining the spatio-temporal evolution and characteristics of large-scale European droughts. BHS Third International Symposium. Managing Consequences of a Changing Global Environment, Newcastle, pp 1–8
- Potop, V., and Mozny, M., (2011). The application of a new drought index- standardized precipitation evapotranspiration index in the Czech Republic, ISBN 978-80-86690-87-2.
- Tayeb Raziei, Isabella Bordi, Luis Santos Pereira. (2011). An application of GPCC and NCEP/NCAR datasets for drought variability analysis in Iran. *Water Resour Manag* 25:1075–1086. DOI <https://doi.org/10.1007/s11269-010-9657-1>.
- Shah, R.; Bharadiya, B.; Manekar, M., (2015). Drought index computation using standardized precipitation index (SPI) method for Surat District, Gujarat, International Conference on Water Resources, Coastal and Ocean Engineering (ICWRCOE 2015) 1243 – 1249
- Sheffield, J., Wood, E. F., (2011). Drought: past problems and future scenarios. P. Earthscan, Ed.
- Shokoohi A, Morovati R (2014) An investigation on the Urmia Lake Basin drought using RDI and SPI indices. *Journal of Watershed Engineering and Management* 6(3):232–246. <https://doi.org/10.22092/jjwmse.2014.101628>
- Singh VP, Guo H, Yu FX (1993) Parameter estimation for 3-parameter log- logistic distribution (LLD3) by Pome. *Stoch Hydrol Hydraul* 7: 163–177
- Stagge JH, Tallaksen LM, Gudmundsson L, Van Loon AF, Stahl K (2015) Candidate distributions for climatological drought indices (SPI and SPEI). *Int J Climatol*. Wiley Online Library 35(13): 4027–4040
- Tallaksen LM, Van Lanen HAJ (2004) Hydrological drought - processes and estimation methods for streamflow and groundwater. In: Tallaksen LM, Van Lanen HAJ (eds) *Developments in Water Sciences*, vol 48. Elsevier B.V., Amsterdam
- Tomros T, Menzel L (2014) Addressing drought conditions under current and future climates in the Jordan River region. *Hydrol Earth Syst Sci* 18:305–318
- Tao H, Gemmer M, Bai YG, Su B, Weiyi M (2011) Trends of streamflow in the Tarim River Basin during the past 50 years: human impact or climate change? *J Hydrol* 400:1–9. <https://doi.org/10.1016/j.jhydrol.2011.01.016>
- Um J, Kim M, Park Y, Kim D, Jeongbin (2017) Effects of different reference periods on drought index (SPEI) estimations from 1901 to 2014. *Hydrol Earth Syst Sci* 21:4989–5007
- Vicente-Serrano SM, Beguería S, López-Moreno JI (2010) A multi-scalar drought index sensitive to global warming: the standardized precipitation evapotranspiration index (SPEI). *J Clim* 23(7):1696–1718
- Vicente-Serrano SM, Beguería S, Lorenzo-Lacruz J et al (2012) Performance of drought indices for ecological, agricultural, and hydrological applications. *Earth Interact* 16(10):1–27
- World Meteorological Organization (WMO) (2006) Drought Monitoring and Early Warning: Concepts, Progress, and Future Challenges, No: 1006. <http://www.wamis.org/agm/pubs/brochures/WMO1006e.pdf>
- Xu K, Yang DW, Yang HB et al (2015) Spatio-temporal variation of drought in China during 1961–2012: a climatic perspective. *J Hydrol* 526:253–264
- Ziese M, Schneider U, Meyer-Christoffer A, Schamm K, Vido J, Finger P, Bissolli P, Pietzsch S, Becker A (2014) The GPCC drought index – a new, combined and gridded global drought index. *Earth Syst Sci Data* 6:285–295

Publisher's note Springer Nature remains neutral with regard to jurisdictional claims in published maps and institutional affiliations.